International Journal of Scientific Research and Engineering Development-– Volume 9 Issue 6, Nov – Dec 2026
Available at www.ijsred.com

RESEARCH ARTICLE OPEN ACCESS

Complementary Seismic Performance of Hybrid Damping Systems in Frames, Wall-Frames and Isolated Bridges under Far-Field, Near-Fault and Long-Duration Ground Motions

Vinod Tiwari[*1], Dr.Shelar Abhay Baburao[*2], Dr. Manoj Sharma[*3]
[*1] Assistant Professor, Department of Civil Engineering
[*2] Associate Professor, Department of Civil Engineering
[*3] Associate Professor, Department of Civil Engineering

----------**********----------

Abstract:

Hybrid damping systems combine mechanically unlike energy-dissipation paths so that each controls a seismic demand the other leaves uncontrolled, yet most published studies compare a hybrid only with the unequipped structure and therefore cannot show that the second path adds anything. This paper evaluates the complementary action of four hybrid assemblies—a parallel viscous–metallic (VM) brace, a friction–viscoelastic (FV) stack, a self-centring (SC) brace with a yielding fuse, and an isolation-plus-damper plane—by comparing each against its own single-mechanism parents with the first-path coefficient held constant. Nonlinear models of four prototypes designed to IS 1893 Zone IV (an eight-storey RC frame, an eight-storey steel frame, a twenty-storey RC wall-frame and a three-span isolated highway bridge) were analysed in OpenSees under separate far-field, near-fault pulse and long-duration record suites, followed by parametric, property-bound, incremental dynamic and second-shock analyses. On the RC frame the VM hybrid at a force-share of 0.70 reduced far-field median peak drift from 1.85 % to 0.92 % (24 % below the better parent) and pulse residual drift from 0.85 % to 0.38 %, while the SC brace reduced residual drift to 0.12 %. Complementarity was class-dependent and index-specific: base shear rose for every equipped frame, and the hybrid benefit appeared as coupling-beam travel on the wall-frame and as bearing stroke (−26 %) and residual offset (−66 %) on the bridge. Force-share, engagement threshold and placement were found to be non-interchangeable design variables. A stepwise design procedure is proposed.

Index Terms—*Hybrid damping, viscous–metallic damper, self-centring brace, base isolation, near-fault ground motion, residual drift, nonlinear response history analysis, performance-based design.*

----------**********----------

1. Introduction

The concept of "capacity design" is used in the earthquake-resistant design in India and other parts of the world, where beams are made to be yielding to absorb energy while columns and foundations are elastic [1, 2]. They collapse without being completely demolished, but they are damaged and may be permanently moved. Each type of supplemental damping device requires the sensing of one kinematic variable: fluid viscous dampers sense velocity but leave residual drift uncorrected [3]–[5]; metallic fuses sense displacement but leave plastic offset; and isolation reduces force but requires large strokes of the bearings under near-fault pulses [6]–[8].

The hybrid damping systems combine two such damping systems, in which each complements or enhances the other's weakness [11, 12]. Viscous–metallic and BRB–viscous frames [13]–[14], self-centring systems with combined dissipation [15]–[17] and isolation planes with dampers [18]–[20] have shown promising reductions. There are three weaknesses in this literature, however. First of all, the hybrid is typically contrasted with the un-equipped structure, which is a demonstration of supplementation not complementarity. Second, results are rarely reported as a function of ground-motion class, but the effect of near-fault pulses is distinctly different from that of long-duration records. Third, steel frames are the dominant and RC frames, wall-frames and highway overpasses are seldom analyzed together.

1) The aim of this study, based on the first author's PhD thesis project, is tackling these deficiencies by conducting a numerical investigation of four hybrid assemblies on four structural prototypes. The goals and impacts are:
2) To determine the gain of each hybrid over its corresponding parent devices when the motion of the first path is fixed for far-field, near fault pulse and long duration motions.
3) Identify the response index for each structural typology that is hybrid, and residual drift as a separate performance claim.
4) To map the effect of force-share, engagement threshold, placement and connection stiffness and test robustness of properties bounds, incremental intensity and second shock.
5) To suggest a step-wise design & checking mechanism as applicable for Indian practice.

 ©IJSRED: All Rights are Reserved

2. Related Work

Makris and Chang demonstrated that the pulse-induced displacement would decrease when friction type force at the isolation plane, but offset would remain, and that it is recommended to use low friction with viscous force [18]. Vargas and Bruneau determined that the viscous damping of the fused systems result in a reduction in drift, and that the strength of the fuse is important to the benefit [13]. Marshall and Charney used a combination of buckling-restrained braces and the viscous or high damping rubber devices in a nine-storey steel frame, and saw that the hybrid performed better on various other indices, despite increasing drift [14]. Self-centring connections and braces have near zero residual drift [21]–[23] and recent studies have developed a combination of self-centring and fluid viscous braces to control residual drift and acceleration [17], [24]. The viscoelastic–friction hybrid devices have been proposed for RC frames in Indian studies [25]. The comparison of multiple hybrid families to their own parents in various typologies and motion classes of hosts is not covered in any of these studies, and is what is addressed here.

3. Methodology

3.1 Research Design

The research design is briefly summarized in Fig 1. The selection of hybrid assemblies and their constitutive laws was taken from the literature, their numerical modeling of four prototypes was performed, and they were then analyzed by nonlinear static analysis and response-history analysis. In three studies, performance indices were then compared in a confirmatory comparison against the parents, a parametric study of design variables, and robustness checks. Multi-objective optimisation of the results led to a design procedure.

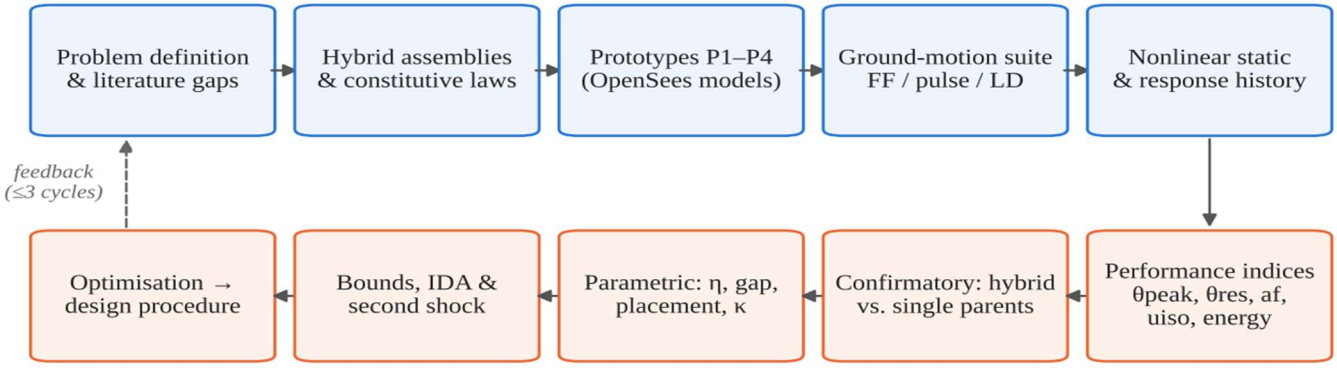

Fig. 1. Research-design flowchart linking problem definition, modelling, analysis, evaluation and development of the design procedure.

3.2 Hybrid Assemblies and Constitutive Models

Four mixed assemblies were kept (Table I). Fluid path: nonlinear viscous law (1); metallic path: bilinear hysteretic law (2); self-centring brace is preloaded restoring element added to fuse, to form a flag shaped loop.

$$Fv = C\,|v|\alpha\,\mathrm{sgn}(v) \quad (1)$$

$$Fh = k0u \text{ for } |u| \le uy;\quad Fh = \pm Fy + r\,k0(u \mp uy) \text{ otherwise} \quad (2)$$

where C is the damping coefficient, v the relative velocity, α the velocity exponent, k0 the initial stiffness, uy the yield displacement, and Fy the yield force, and r the post-yield stiffness ratio. The force-share η is a ratio of the two paths, and the initiation of the second path is indicated by the engagement threshold (ug/Δd) normalised by design storey drift Δd:

$$\eta = \frac{F2}{F1}, \text{re} \quad (3)$$

where F2 is the characteristic force of the second mechanism and F1,ref the force of the first mechanism at the design storey drift or design isolator displacement. If there is a force-share of zero, the single-parent reference is recovered. In the case of the self-centring brace, the ratio λr of dissipative to restoring force takes the place of the same ratio.

TABLE I HYBRID ASSEMBLIES AND DESIGN VARIABLES

Assembly	First path	Second path	Variables examined (nominal)
Viscous–metallic (VM) brace	Fluid damper, C, α	Metallic fuse, F_y, r	η (0.70), u_g/Δ_d (0), placement
Friction–viscoelastic (FV) stack	Viscoelastic pad (stiffness, loss)	Friction interface, slip force F_s	η (0.70), slip threshold
Self-centring (SC) brace	Preloaded restoring element	Yielding / friction fuse F_d	$\lambda_r = F_d/F_{restore}$ (0.90)
Isolation + damper	Isolation bearings (T_{iso})	Supplemental viscous dampers	η (0.70), recomputed from T_{iso}

 ©IJSRED: All Rights are Reserved

3.3 Prototype Structures

Four prototypes were designed for IS 1893 (Part 1): 2016 Zone IV (Medium soil) (Table II). P1 and P2 are eight-story moment frames with hybrid braces in the exterior bays, while P3 is a two-by-two-span highway overpass in which dampers are used in parallel with the isolation bearings at both interior columns, but the coupling beams in the lower twenty storeys are replaced by hybrid braces. OpenSees [26] models were created using fibre beam–column elements and rigid floor diaphragms and connection springs at brace to joint connections. The Newmark average-acceleration method was used for time integration.

TABLE II GEOMETRY, MASS AND MODAL PROPERTIES OF THE PROTOTYPES

Prototype	Configuration	Seismic weight (kN)	T_1 bare / equipped (s)
P1 – mid-rise RC frame	8 storeys, 3 × 3 bays of 9 m, H = 28 m	48 600	1.12 / 0.98
P2 – mid-rise steel frame	8 storeys, 3 × 3 bays of 9 m, H = 28 m	32 400	1.35 / 1.08
P3 – tall RC wall-frame	20 storeys, coupled walls, H = 70 m	186 000	2.40 / 2.15
P4 – isolated highway bridge	Spans 30–40–30 m, RC piers 10 m	24 800 (deck)	1.55 isolated / 1.22 with dampers

3.4 Ground-Motion Suite

The three record classes were put together in such a way that none of the classes represents another [27]. The far field class has seven records of earthquakes (Mw 6.5–7.6, rupture distance>10 km) in Imperial Valley, Northridge, Loma Prieta, Düzce, Chi-Chi, Hector Mine and San Fernando. The near fault class consists of seven records, each with a unique velocity pulse as follows: El Centro Array #6, Rinaldi, Sylmar, Takatori, Lucerne and TCU068. The long-duration class comprises four subduction records from Maule 2010, Tohoku 2011 and Valparaíso 1985. The records were amplitude scaled to IS 1893 Zone IV, soil type II spectrum limited to 0.4 to 2.5, for isolated models, limited to 0.75T1 to 1.25T1. Horizontal components and the vertical components were given to P4 and the isolated variant of P1.

3.5 Analysis Procedure and Performance Indices

Gravity analysis, modal analysis, first-mode pushover and response-history analysis were performed for each of the three models. Reported indices are the peak inter-storey drift θpeak, the residual drift θres, peak floor acceleration af, base-shear ratio Vb/W, isolator stroke and the path-wise energy ratio of (4). The ratio of recentring, defined in (5), is recent.

$$\rho_E = E_{h,2} / (E_{h,1} + E_{h,2}) \quad (4)$$

$$R_c = \theta_{res} / \theta_{peak} \quad (5)$$

If a hybrid's second path dissipated less than 10 % of the device energy (ρE < 0.10) on a record, then the hybrid was redefined as a single-parent system for that record. Indicative acceptance bands were 2.0 % peak drift for life safety, 0.5 % residual drift for repairability and 0.4 g floor acceleration for non-structural screening. Robustness was evaluated using upper bound, lower bound and mixed property surfaces, incremental dynamic analysis [29] and a second shock at half the design level.

4. Results and Discussion

4.1 Modal and Static Response

The first-mode period for P1 was reduced from 1.12 s to 0.98 s (Table II) and that for P2 was reduced from 1.35 s to 1.08 s (Table II) with first-mode participating mass kept above 70 %. With isolation, the P1 period increased to 2.41 s and with supplemental dampers, it decreased to 2.18 s. The pushover analysis resulted in the following hierarchy: hybrid fuses would blow first before beams and there was no yielding of columns below 2.2 % roof drift on P1.

4.2 Peak Inter-Storey Drift of the RC Frame

Fig. 2 shows the differences of peak drift between the P1 in three motion classes. With far-field motion, the unequipped median was lowered by 1.85 % to 1.21 % due to the viscous parent, 1.16 % due to the metallic parent, and 0.92 % due to the VM hybrid—a decrease of 24 % compared to the better parent and 50 % compared to the bare frame. The pulse class changed the ranking of the parents: the metallic (1.72 %) parent consistently outperformed the viscous (1.94 %) parent, as a path with a displacement dependence is used during a long period pulse, and the time spent at high velocity is short. The metallic parent was 1.35 %, a little better than the hybrid. In the long duration motion, all the fluid path models improved, with the VM hybrid achieving the lowest value of 0.88 %. A reduction not accompanied by its motion class would then give a false impression of the rankings of two of the three classes.

 ©IJSRED: All Rights are Reserved

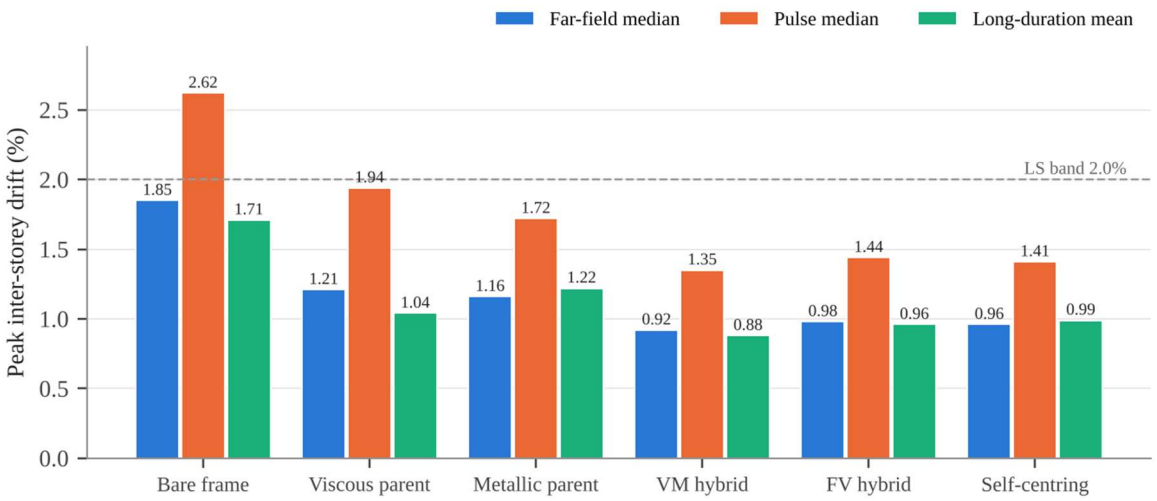

Fig. 2. Peak inter-storey drift of prototype P1 by model and motion class (far-field and pulse medians, long-duration mean). The dashed line marks the 2.0 % life-safety interpretive band.

4.3 Residual Drift and Floor Acceleration

Residual drift was responsible for the separation of assemblies that had peak drift near together (Fig. 3(a)). With the pulse class the bare frame remained at 0.85 %, the viscous parent at 0.74 % and the metallic parent at 0.72 %; with the VM and FV hybrids it was 0.38 % and with the SC brace, only 0.12 % – the only assembly within a 0.2 % band at each storey. The ratios of recentring were 0.42 for the metallic parent, 0.28 for the VM hybrid and 0.09 for the SC brace, indicating that the residual drift decreased more rapidly than the peak drift. Roof acceleration (Fig. 3(b)) behaved differently, however: the metallic parent increased it from 0.47 g to 0.54 g, while the viscous parent decreased it to 0.36 g, and the hybrid took half the viscous benefit, at 0.41 g.

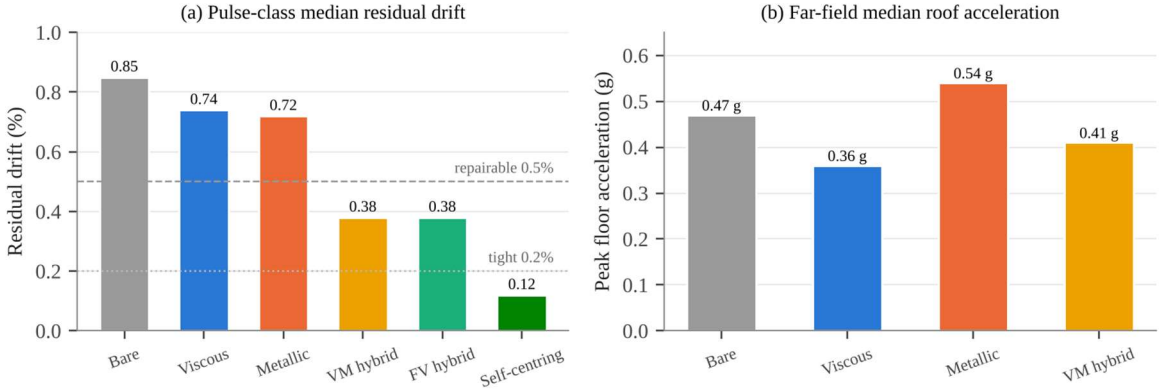

Fig. 3. Prototype P1: (a) pulse-class median residual inter-storey drift with repairable (0.5 %) and tight (0.2 %) bands; (b) far-field median roof acceleration.

4.4 Hybrid versus Parent Devices

The VM hybrid for P1 is shown as median ratios to each parent in Fig. 4. The hybrid increased the roof acceleration by 1.14 and base shear by 1.24, and decreased the far field drift by 0.76, the pulse drift by 0.70 and the pulse residual drift by 0.51 as compared with the viscous parent. It decreased roof acceleration from 0.86 to 0.76, and residual drift from 0.6 to 0.53, while only increasing base shear to 1.06 against the metallic parent. Thus, one who values only farfield drift would be able to use either parent, but one who values residual drift and acceleration would not. This was repeated, albeit to a lesser extent with the FV stack, with a 0.48 % to 0.38 % pulse residual drift and a 1.17 % to 0.98 % far field drift (pad only). The fluid path was taken under the far-field and long-duration records and the fuse under the pulses, which confirmed that both paths were working correctly in the VM unit.

 ©IJSRED: All Rights are Reserved

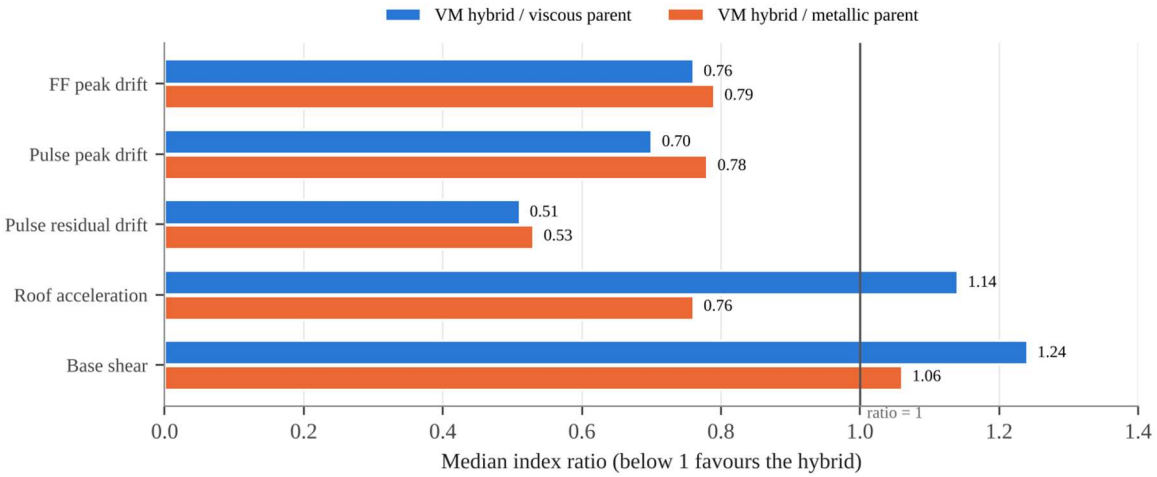

Fig. 4. Median index ratios of the viscous–metallic hybrid of P1 to each single-parent reference; a ratio below one favours the hybrid.

4.5 Other Structural Typologies

The other prototypes are summarised in Table III. On the steel frame P2 the VM hybrid resulted in a reduction in far-field drift of 53 % and a reduction in pulse residual drift from 0.96 % to 0.41 % which were the same as the P1 results. The benefit was evident in the coupling-beam travel and mid-height acceleration, not in roof acceleration, on the wall-frame P3, since the hybrid zone was only built to the twelfth floor. However, on the bridge P4, isolation alone resulted in a pulse median stroke of 236 mm, which is larger than the design displacement of 180 mm, while the pulse median stroke was reduced by 15 % with dampers and the residual offset was reduced by 66 % at the expense of 15 % higher pier drift and 28 % higher deck acceleration. A universal drift reduction recommendation would have thus described 3 of the 4 hosts.

TABLE III MEDIAN RESPONSE OF P2, P3 AND P4 WITHOUT AND WITH HYBRID DAMPING

Prototype	Index (class)	Without hybrid	With hybrid
P2 steel frame	θ_{peak} far-field (%)	2.08	0.97
P2 steel frame	θ_{peak} pulse (%)	2.94	1.48
P2 steel frame	θ_{res} pulse (%)	0.96	0.41
P3 wall-frame	Peak wall drift far-field (%)	0.76	0.55
P3 wall-frame	Storey-10 acceleration far-field (g)	0.38	0.29
P3 wall-frame	Coupling-beam travel pulse (mm)	24.6	16.4
P4 bridge	Isolator stroke far-field (mm)	142	108
P4 bridge	Isolator stroke pulse, median / 84th (mm)	236 / 312	174 / 228
P4 bridge	Pier drift pulse (%)	0.34	0.39

4.6 Force-Share, Threshold, Placement and Connection Stiffness

Fig. 5 plots VM unit of P1 against the force-share and engagement threshold. The drift in the far-field increased from 1.04 % to 0.92 % as η increased from 0.35 to 0.70, and even larger gains were obtained when further increased to 1.00, resulting in the drift of the device force being closer to the joint capacity. At 0.25Δd, both indices remained essentially the same, but at 0.75Δd the energy share in the far field for the fuse decreased to 0.11, and in the case of long duration motion, the hybrid was effectively retransformed into its viscous parent. The larger the fuse the larger the gap. Lower-storey-only placement resulted in creation of new peak in the first unequipped storey and this placement was rejected; full-height placement was the default, and mixed placement (viscous units above, hybrid braces below) was preferred if the roof acceleration is a target. A soft connection with stiffness only 5 times of the initial device stiffness resulted in the device seeing 74% of the brace elongation which in turn increased the far-field drift from 0.92% to 1.14 %.

 ©IJSRED: All Rights are Reserved

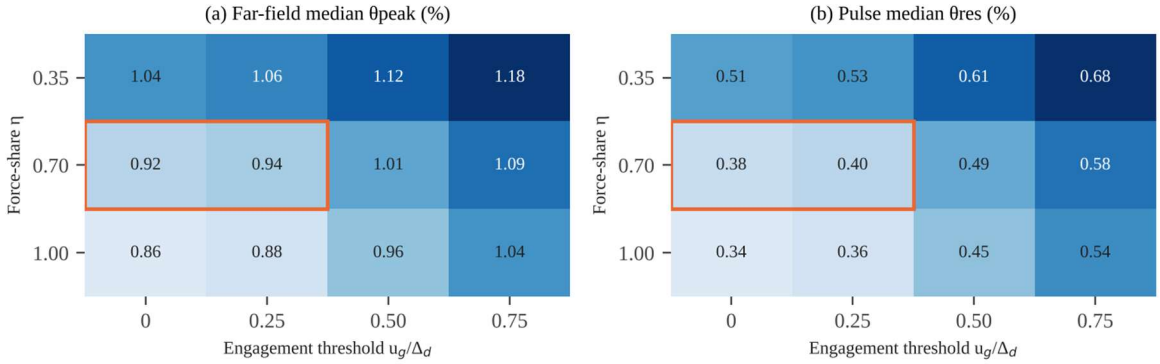

Fig. 5. Force-share–threshold matrix for the viscous–metallic unit of P1: (a) far-field median peak drift; (b) pulse median residual drift. The outlined cells (η = 0.70, threshold 0–0.25) form the recommended default.

4.7 Robustness under Property Bounds, Increasing Intensity and Aftershock

The VM hybrid outperformed both parents on all upper-bound, lower-bound and mixed property surfaces in terms of far-field peak drift, and held the edge on the lower-bound and weak-fuse surfaces. The hybrid advantage remained and increased under pulses as demonstrated by incremental dynamic analysis showing that the bare frame exceeded the 5 % drift limit on three out of four pulse records, whereas the hybrid limit was not exceeded in the range of analysis. The VM residual had only a slight increase of 0.03-0.05 percentage points after a second shock at half the design level, and the SC brace was not even exceeded by 0.2 %.

5. Proposed Design Procedure

The results were summarised in an Indian practice checking sequence for hybrid damping:

1) Design the host frame according to capacity principles as per IS1893, do not compromise the size of the members due to the devices.
2) Governing target: VM brace (for peak drift), SC brace (for residual target less than 0.5 %), isolation plus dampers for stroke-governed bridges.
3) Calculate F1,ref for the equipped or isolated period, using η = 0.70, exterior-bay placement with no gap and full height.
4) Conduct far field and pulse suites (at least seven records each) and a long duration set when warranted by the site.
5) Measure peak drift, residual drift, floor acceleration, device energy share (ρE ≥ 0.10), joint or pier force at maximum 84th percentile pulse demand, connection stiffness (at least ten times device stiffness).
6) Adjust within 3 cycles: drift adjustment (placement or small η adjustment), change to an SC brace (residual drift), placement (mixed)..

6. Conclusions

A total of four hybrid damping assemblies were tested on four structural prototypes under three different ground-motion classes, where each hybrid was tested against its own parent damping device. The main conclusions are:

1. An additional path of dissipation that is non-controllable by its parent, the VM hybrid in the RC frame actually decreased the far-field peak drift by 50 % (24 % beyond the better parent frame) and the pulse residual drift by 55 % while base shear was increased for all of the frames equipped with the VM hybrid.
2. Complementarity was class-dependent, with the order of the parent classifications switching between far field and pulse motion, and reductions should always be reported in conjunction with the motion class.
3. Residual drift is an independent performance claim – only the self-centring brace was able to achieve a 0.2 % target, and a fuse level increase did not compensate for lack of restoring path.
4. Index used to receive hybrid benefit varied by typology: storey drift (used for frames); coupling-beam travel and mid-height acceleration (used for wall-frame); stroke and residual offset (used for isolated bridge).
5. Force-share, engagement threshold, placement and connection stiffness are independent design variables; η = ~0.70 with the threshold of no more than 0.25Δd is a strength default; full-height placement is a strength default.

The study is numerical and the device laws have been extracted from published parent calibrations; shake-table testing of integrated hybrid packages and connections and calibration of the procedure for irregular buildings and liquefiable sites are recommended for future studies.

References

[1] Bureau of Indian Standards, *Criteria for Earthquake Resistant Design of Structures, Part 1: General Provisions and Buildings*, IS 1893 (Part 1): 2016, New Delhi, India, 2016.

[2] American Society of Civil Engineers, *Minimum Design Loads and Associated Criteria for Buildings and Other Structures*, ASCE/SEI 7-22, Reston, VA, USA, 2022, doi: 10.1061/9780784415788.

[3] G. W. Housner *et al.*, "Structural control: Past, present, and future," *J. Eng. Mech.*, vol. 123, no. 9, pp. 897–971, 1997, doi: 10.1061/(ASCE)0733-9399(1997)123:9(897).

[4] T. T. Soong and B. F. Spencer Jr., "Supplemental energy dissipation: State-of-the-art and state-of-the-practice," *Eng. Struct.*, vol. 24, no. 3, pp. 243–259, 2002, doi: 10.1016/S0141-0296(01)00092-X.

[5] M. D. Symans *et al.*, "Energy dissipation systems for seismic applications: Current practice and recent developments," *J. Struct.*

 ©IJSRED: All Rights are Reserved

Eng., vol. 134, no. 1, pp. 3–21, 2008, doi: 10.1061/(ASCE)0733-9445(2008)134:1(3).

[6] W.-H. Lin and A. K. Chopra, "Earthquake response of elastic SDF systems with non-linear fluid viscous dampers," *Earthq. Eng. Struct. Dyn.*, vol. 31, no. 9, pp. 1623–1642, 2002, doi: 10.1002/eqe.179.

[7] K.-C. Tsai, H.-W. Chen, C.-P. Hong, and Y.-F. Su, "Design of steel triangular plate energy absorbers for seismic-resistant construction," *Earthq. Spectra*, vol. 9, no. 3, pp. 505–528, 1993, doi: 10.1193/1.1585727.

[8] A. Javanmardi, Z. Ibrahim, K. Ghaedi, H. Benisi Ghadim, and M. U. Hanif, "State-of-the-art review of metallic dampers: Testing, development and implementation," *Arch. Comput. Methods Eng.*, vol. 27, no. 2, pp. 455–478, 2020, doi: 10.1007/s11831-019-09329-9.

[9] R. S. Jangid and J. M. Kelly, "Base isolation for near-fault motions," *Earthq. Eng. Struct. Dyn.*, vol. 30, no. 5, pp. 691–707, 2001, doi: 10.1002/eqe.31.

[10] J. F. Hall, T. H. Heaton, M. W. Halling, and D. J. Wald, "Near-source ground motion and its effects on flexible buildings," *Earthq. Spectra*, vol. 11, no. 4, pp. 569–605, 1995, doi: 10.1193/1.1585828.

[11] T. E. Saaed, G. Nikolakopoulos, J.-E. Jonasson, and H. Hedlund, "A state-of-the-art review of structural control systems," *J. Vib. Control*, vol. 21, no. 5, pp. 919–937, 2015, doi: 10.1177/1077546313478294.

[12] M. H. Stanikzai, S. Elias, and Y. Chae, "Recent advances in hybrid vibration-control systems," *Pract. Period. Struct. Des. Constr.*, vol. 27, no. 3, Art. no. 03122003, 2022, doi: 10.1061/(ASCE)SC.1943-5576.0000685.

[13] R. Vargas and M. Bruneau, "Effect of supplemental viscous damping on the seismic response of structural systems with metallic dampers," *J. Struct. Eng.*, vol. 133, no. 10, pp. 1434–1444, 2007, doi: 10.1061/(ASCE)0733-9445(2007)133:10(1434).

[14] J. D. Marshall and F. A. Charney, "Seismic response of steel frame structures with hybrid passive control systems," *Earthq. Eng. Struct. Dyn.*, vol. 41, no. 4, pp. 715–733, 2012, doi: 10.1002/eqe.1153.

[15] W. Y. Kam, S. Pampanin, A. Palermo, and A. J. Carr, "Self-centering structural systems with combination of hysteretic and viscous energy dissipations," *Earthq. Eng. Struct. Dyn.*, vol. 39, no. 10, pp. 1083–1108, 2010, doi: 10.1002/eqe.983.

[16] R. Tremblay, M. Lacerte, and C. Christopoulos, "Seismic response of multistory buildings with self-centering energy dissipative steel braces," *J. Struct. Eng.*, vol. 134, no. 1, pp. 108–120, 2008, doi: 10.1061/(ASCE)0733-9445(2008)134:1(108).

[17] C. Qiu, L. Cheng, and X. Du, "Seismic design of hybrid braced frames with self-centering braces and fluid viscous damping braces," *Eng. Struct.*, vol. 280, Art. no. 115728, 2023, doi: 10.1016/j.engstruct.2023.115728.

[18] N. Makris and S.-P. Chang, "Effect of viscous, viscoplastic and friction damping on the response of seismic isolated structures," *Earthq. Eng. Struct. Dyn.*, vol. 29, no. 1, pp. 85–107, 2000, doi: 10.1002/(SICI)1096-9845(200001)29:1<85::AID-EQE902>3.0.CO;2-N.

[19] C. P. Providakis, "Effect of LRB isolators and supplemental viscous dampers on seismic isolated buildings under near-fault excitations," *Eng. Struct.*, vol. 30, no. 5, pp. 1187–1198, 2008, doi: 10.1016/j.engstruct.2007.07.020.

[20] A. A. Mazloum, M. Amin Afshar, and S. Aghaeipour, "Seismic assessment of isolator-damper hybrid structural system based on analysis of MDOF and modal 2DOF models," *Structures*, vol. 58, Art. no. 105571, 2023, doi: 10.1016/j.istruc.2023.105571.

[21] J. M. Ricles, R. Sause, M. M. Garlock, and C. Zhao, "Posttensioned seismic-resistant connections for steel frames," *J. Struct. Eng.*, vol. 127, no. 2, pp. 113–121, 2001, doi: 10.1061/(ASCE)0733-9445(2001)127:2(113).

[22] C. Christopoulos, R. Tremblay, H.-J. Kim, and M. Lacerte, "Self-centering energy dissipative bracing system for the seismic resistance of structures: Development and validation," *J. Struct. Eng.*, vol. 134, no. 1, pp. 96–107, 2008, doi: 10.1061/(ASCE)0733-9445(2008)134:1(96).

[23] J. Erochko, C. Christopoulos, and R. Tremblay, "Design, testing, and detailed component modeling of a high-capacity self-centering energy-dissipative brace," *J. Struct. Eng.*, vol. 141, no. 8, Art. no. 04014193, 2015, doi: 10.1061/(ASCE)ST.1943-541X.0001166.

[24] S. Hu, C. Qiu, and S. Zhu, "Machine learning-driven performance-based seismic design of hybrid self-centering braced frames with SMA braces and viscous dampers," *Smart Mater. Struct.*, vol. 31, no. 10, Art. no. 105024, 2022, doi: 10.1088/1361-665X/ac8efc.

[25] M. B. Addala, S. Bhalla, and A. Madan, "Controlling dynamic response of structures using hybrid passive energy dissipation device," *J. Earthq. Eng.*, pp. 1–19, 2020, doi: 10.1080/13632469.2020.1792378.

[26] F. McKenna, G. L. Fenves, and M. H. Scott, "Nonlinear finite-element analysis software architecture using object composition," *J. Comput. Civ. Eng.*, vol. 24, no. 1, pp. 95–107, 2010, doi: 10.1061/(ASCE)CP.1943-5487.0000002.

[27] I. Iervolino and C. A. Cornell, "Record selection for nonlinear seismic analysis of structures," *Earthq. Spectra*, vol. 21, no. 3, pp. 685–713, 2005, doi: 10.1193/1.1990199.

[28] J. W. Baker, "Quantitative classification of near-fault ground motions using wavelet analysis," *Bull. Seismol. Soc. Am.*, vol. 97, no. 5, pp. 1486–1501, 2007, doi: 10.1785/0120060255.

[29] D. Vamvatsikos and C. A. Cornell, "Incremental dynamic analysis," *Earthq. Eng. Struct. Dyn.*, vol. 31, no. 3, pp. 491–514, 2002, doi: 10.1002/eqe.141.

 ©IJSRED: All Rights are Reserved